

# Calculations of Dielectric Loaded Traveling-Wave Periodic Structure Properties

Peng Zou Liling Xiao Xiang Sun Wei Gai Thomas Wong\*

*Argonne National Laboratory, Argonne, IL60439  
\*Also Illinois Institute of Technology, Chicago, IL60616*

**Abstract.** One disadvantage of conventional iris-loaded accelerating structures is the high ratio of peak surface electric field to peak axial electric field. It limits the maximum achievable accelerating gradient to less than one half of the electric surface breakdown limit at the operating frequency, if the required high power RF sources are always available. Such high ratio of peak surface electric field to peak axial electric field becomes a hurdle for realizing an accelerator technology with very high accelerating gradient, which is very important for the next generation linear collider. One way to overcome this hurdle is to design a new structure that has a small ratio of peak surface electric field to accelerating gradient, while the shunt impedance per unit length  $r$  and  $Q$  do not scarify much. We present a scheme with dielectric-loaded periodic structures to achieve these objectives. The analyses based on MAFIA simulations of such kind of structure show that we can lower the peak surface electric field close to the accelerating gradient with high acceleration efficiency that is measured by  $r/Q$ . Meanwhile, the shunt impedance and  $Q$  of such structure is comparable with conventional pure iris-loaded accelerating structures. Thus the maximum achievable accelerating gradient in dielectric-loaded periodic structures can be at least the double of that of conventional iris-loaded accelerating structures.

## I. INTRODUCTION

It is generally agreed that the next generation linear collider must use an affordable and compact accelerator technology. A very high axial peak electric field gradient can certainly deliver the required energy to a particle within very short distance. However, the peak surface electric field is an important constraint in such high-energy accelerating structure design. In normal-conducting cavities, too large a peak surface electric field can result in electric breakdown. For conventional iris-loaded traveling-wave accelerators, the typical ratio of peak surface electric field  $E_s$ , which occurs at the edges of irises, to the peak axial electric field  $E_{z0}$  is generally greater than 2. If the peak surface electric field exceeds the breakdown limit at the operating frequency, it can cause arcing damages to irises. Thus the high ratio of peak surface electric field to peak axial electric field is a hurdle for achieving high accelerating gradient. Assuming the availability of high power RF sources is not a problem here, the maximum achievable accelerating gradient is always less than one half of the electric surface

breakdown limit at the operating frequency in a pure iris-loaded structure. If the ratio of  $E_s/E_{z0}$  can be reduced to about 1, without losing too much acceleration efficiency that is measured by shunt impedance  $r$  and  $r/Q$ , the maximum achievable accelerating gradient can be increased dramatically. As a natural corollary, it is of great interest to study some new structures that have lower ratio of  $E_s/E_{z0}$ , and comparable shunt impedance per unit length and  $r/Q$  with conventional iris-loaded accelerating structures.

The advantages of using dielectric-lined circular waveguides as accelerating structures have been discussed in many previous studies [1-4]. One distinguished benefit is that the accelerating axial electric field is the maximum in such kind of structure, while the peak surface electric field is zero. Nevertheless, a good accelerating structure requires the group velocity of  $TM_{01}$  mode less than 10 percent of the speed of light in the free space. Then we have to fill waveguides with high-dielectric-constant ceramics. One drawback of using high dielectric constant materials is the largely increased peak surface magnetic field, which causes more power dissipation on the wall. Thus the higher dielectric constant, the lower the quality factor  $Q$  of such structure. In addition to this, dielectric ceramics with higher dielectric constant are relatively more expensive and lossy.

Loading dielectric will change field distributions of waveguides. Meanwhile, iris-loaded structures can efficiently slow group velocity with very high  $Q$ . Thus we may be able to strike a balance between the advantages of these two kinds of structures by using a combination of them with low-dielectric-constant materials. Fig. 1 shows such dielectric-iris-loaded structure. Calculations of such structure will show that it can significantly reduce the ratio of the peak surface electric field to the peak axial electric field without scarifying much in shunt impedance per unit length  $r$  and  $r/Q$ .

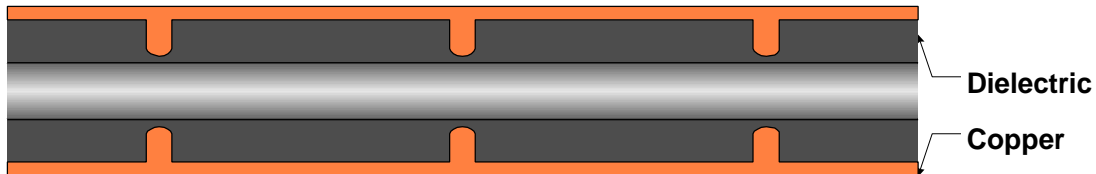


**FIGURE 1.** Schematic drawing of dielectric-iris-loaded accelerating structure.

## II. BASIC EQUATIONS

Our calculation will limit to X-band traveling-wave structures. For X-band and higher frequency band accelerators, traveling-wave structures are preferred to standing-wave structures, because they are less expensive in fabrication, and high power RF isolators or circulators that are necessary for standing-wave accelerators are not currently available in X-band and higher frequency band. As mentioned above, periodic iris-loaded structures are viewed as arrays of pillboxes coupled through irises. Such kind of standing-wave structure can be accurately calculated as a resonator using electromagnetic field-solving codes such as eigenmode module of MAFIA, and SuperFish. Previous calculations of disk-loaded accelerating structures showed how

to obtain RF properties of traveling-wave structure from the calculation results of standing-wave structures [5]. This conversion will be briefly visited in the following.

## Space Harmonics, Standing and Traveling Waves

It is well known that the  $E_z$  of  $TM_{01}$  mode in the traveling-wave structures can be expressed as:

$$E_{z,TW} = \sum_{n=-\infty}^{n=+\infty} a_n J_0(k_m r) e^{j(\omega t - b_n z)}. \quad (1)$$

where  $a_n$  is the amplitude of the space harmonic of index  $n$ ,

$$b_n z = b_o z + \frac{2pnz}{d} \quad (2)$$

$k_m^2 = k^2 - b_n^2$ ,  $k = \omega / c$  and  $d$  is the periodic length.

With Neuman boundary condition ( $E_T=0$ ), the axial electric fields of the standing waves can be expressed as:

$$E_{z,SW} = e^{j\omega t} \sum_{n=-\infty}^{n=+\infty} 2a_n \cos b_n z. \quad (3)$$

where the factor of 2 comes from the summation of two traveling waves of amplitude  $a_n$ . This equation is also true to other field components.

## Conversion from Standing Waves to Traveling Waves

Using E-module of MAFIA, one can calculate resonant frequencies, stored energies and dissipated power of resonance modes in the cavities. The field components can also be extracted from such standing-wave simulation results. If two traveling waves of the proper phase add up to a standing wave (Equation (3)), there must conversely be two standing waves that add up to a traveling wave. Assuming the first standing wave is  $\vec{A}$ , and the second standing wave  $\vec{B}$  is shift  $\vec{A}$  to the left by  $d$ , one can have:

$$\begin{aligned} \vec{B} &= e^{j\omega t} \sum_{n=-\infty}^{+\infty} 2a_n \cos b_n (z + d) \\ \vec{A} &= e^{j\omega t} \sum_{n=-\infty}^{+\infty} 2a_n \cos b_n z \end{aligned} \quad (4)$$

Both of these standing waves are made up of one traveling wave going left and one going right. It is possible to add them with the proper phases to have the traveling waves going left canceled and those going right added. Thus, we can obtain the traveling wave field component in such structure. This can be achieved by multiplying  $\vec{A}$  by  $e^{j(b_0 d - p/2)}$  and  $\vec{B}$  by  $e^{jp/2}$ .

$$\begin{aligned} \vec{B} &= e^{j\omega t} \sum_{n=-\infty}^{+\infty} 2a_n \cos b_n (z + d) = e^{j\omega t} \sum_{n=-\infty}^{+\infty} a_n (e^{-jb_n(z+d)} + e^{jb_n(z+d)}) \\ \vec{A} &= e^{j\omega t} \sum_{n=-\infty}^{+\infty} 2a_n \cos b_n z = e^{j\omega t} \sum_{n=-\infty}^{+\infty} a_n (e^{-jb_n z} + e^{jb_n z}) \end{aligned} \quad (5)$$

$$\bar{B}e^{jp/2} = e^{j\omega t} e^{jp/2} \sum_{-\infty}^{+\infty} a_n (e^{-jb_n(z+d)} + e^{jb_n(z+d)}) \quad (6)$$

$$\bar{A}e^{j(b_0d-p/2)} = e^{j\omega t} e^{j(b_0d-p/2)} \sum_{-\infty}^{+\infty} a_n (e^{-jb_nz} + e^{jb_nz})$$

$$\mathbf{b}_nz = \mathbf{b}_0z + 2pnz/d$$

$$\mathbf{b}_nd = \mathbf{b}_0d + 2pn \quad (7)$$

Substituting Equation (7) into (6), we can have

$$\bar{B}e^{jp/2} = e^{j\omega t} \sum_{-\infty}^{+\infty} a_n (je^{jb_nz} e^{jb_0d} + je^{-jb_nz} e^{-jb_0d})$$

$$\bar{A}e^{j(b_0d-p/2)} = e^{j\omega t} \sum_{-\infty}^{+\infty} a_n (-je^{jb_nz} e^{jb_0d} - je^{-jb_nz} e^{jb_0d}) \quad (8)$$

Adding up the two equations in (8), we can have

$$\bar{B}e^{jp/2} + \bar{A}e^{j(b_0d-p/2)} = 2 \sin \mathbf{b}_0d \sum_{-\infty}^{+\infty} a_n e^{j(\omega t - \mathbf{b}_nz)} \quad (9)$$

The amplitude and phase of the field components of traveling waves can be obtained by the following equations:

$$|TW|^2 = \frac{A^2 + B^2 - 2AB \cos \mathbf{b}_0d}{4 \sin^2 \mathbf{b}_0d}$$

$$\tan \mathbf{q}(z) = \frac{B - A \cos \mathbf{b}_0d}{A \sin \mathbf{b}_0d} \quad (10)$$

where A and B are functions of z.

## Group Velocity

For practical cases where the dispersion is not too large, the energy velocity is equal to the group velocity. Thus the group velocity of a traveling wave can be calculated from the energy velocity  $V_g = P/W_{TW}$ , where P the time average power flow and  $W_{TW}$  is the time average energy stored per unit length. For a given z, we have:

$$V_g = \frac{\frac{1}{2} \int \text{Re}(\vec{E}_r \times \vec{H}_f^*) ds}{\int_{\text{unit length}} \left( \frac{\epsilon E^2}{4} + \frac{\mu H^2}{4} \right) dV} \quad (11)$$

## Power And Acceleration Efficiency Figures of Merit

To discuss the design of dielectric loaded accelerating structures, it is helpful to introduce some commonly used figures of merit for accelerating structures and some important considerations in dealing with design issues. Then we can optimize our design choices according to these parameters. Furthermore, the new accelerator technology based on dielectric loaded structure can be merited quantitatively. Here we present the definitions of these parameters for standing-wave structures to clarify

the physics contained within them. These figures of merit of traveling-wave accelerating structures can be derived from those of standing-wave structures. Moreover, our calculations of the traveling-wave structures were obtained from the results of the standing-wave cavities.

There are several figures of merit that are commonly used to characterize accelerating structures. Some of these depend on the power that is dissipated because of electrical resistance in the walls of the cavities. The well-known quality factor of a resonator is one of them. It is defined in terms of the average power loss  $P$  as

$$Q = \frac{\omega U}{P} \quad (12)$$

The shunt impedance, a figure of merit that is independent of the excitation level of the cavity and measures the effectiveness of producing an axial voltage  $V_0$  for a given power dissipated, is defined by

$$r_s = \frac{V_0^2}{P} \quad (13)$$

In an accelerating structure we are really more interested in maximizing the particle energy gain per unit power dissipation. The energy gain of an arbitrary particle with charge  $q$  traveling through the gap on axis of a standing-wave cavity is

$$\Delta W = q \int_{-L/2}^{L/2} E(0, z) \cos[\omega t(z) + \mathbf{f}] dz \quad (14)$$

for the given accelerating gap shown in Fig. 2.1, and the electric field on the axis experienced by this particle with velocity  $v$  as

$$E_z(r=0, z, t) = E(0, z) \cos[\omega t(z) + \mathbf{f}] \quad (15)$$

where  $t(z) = \int_0^z dz/v(z)$  is the time the particle is at position  $z$ . At  $t=0$ , the phase of the field relative to the crest is  $\phi$ .

The use of a common trigonometric identity allows us to write the energy gain as

$$\begin{aligned} \Delta W &= q \int_{-L/2}^{L/2} E(0, z) [\cos \omega t \cos \mathbf{f} - \sin \omega t \sin \mathbf{f}] dz \\ \Delta W &= q V_0 T \cos \mathbf{f} \end{aligned} \quad (16)$$

where  $V_0$  is an axial RF voltage, defined by

$$V_0 \equiv \int_{-L/2}^{L/2} E(0, z) dz \quad (17)$$

The transit-time factor  $T$  is defined by

$$T \equiv \frac{\int_{-L/2}^{L/2} E(0, z) \cos \omega t(z) dz}{\int_{-L/2}^{L/2} E(0, z) dz} - \tan \mathbf{f} \frac{\int_{-L/2}^{L/2} E(0, z) \sin \omega t(z) dz}{\int_{-L/2}^{L/2} E(0, z) dz} \quad (18)$$

The phase  $\phi=0$  if the particle arrives at the origin when the field is at a crest. It is negative if the particle arrives at the origin earlier than the crest, and positive if it arrives later. Maximum energy gain occurs when  $\phi=0$ , which is often the choice for relativistic electrons. The phase and the transit-time factor depend on the choice of the origin. It is convenient to simplify the transit-time factor, and remove its dependence

on the phase, by choosing the origin at the electrical center.  $E(z)$  is usually approximately an even function about a geometric center of the gap. We will choose the origin at the electrical center of the gap, then

$$0 = \int_{-L/2}^{L/2} E(0, z) \sin \omega t(z) dz \quad (19)$$

When  $E(z)$  is an even function about the geometric center of the gap, the electrical center and the geometric center coincide. The transit-time factor simplifies to

$$T \equiv \frac{\int_{-L/2}^{L/2} E(0, z) \cos \omega t(z) dz}{\int_{-L/2}^{L/2} E(0, z) dz} \quad (20)$$

The transit-time factor expression in this equation is the average of the cosine factor weighted by the field. The transit-time factor increases when the field is more concentrated longitudinally near the origin, where the cosine factor is largest. In most practical cases the change of particle velocity in the gap is small compared to the initial velocity. If we ignore the velocity change, we have

$$\omega t \approx \frac{\omega z}{v} = \frac{2\pi z}{bl} \quad (21)$$

where  $b=v/c$  and  $bl$  is the distance the particle travels in an RF period. Then, the simplified form of the transit-time factor most often used is defined by

$$T \equiv \frac{\int_{-L/2}^{L/2} E(0, z) \cos(2\pi z / bl) dz}{\int_{-L/2}^{L/2} E(0, z) dz} \quad (22)$$

The average axial electric-field amplitude is defined by  $E_0=V_0/L$ , where  $V_0$  is the voltage gain that would be experienced by a particle passing a constant dc field equal to the field in the gap at time  $t=0$ . The accelerating gradient is the quantity  $E_0T$ . In terms of  $E_0$ , the energy gain can be expressed by the Panofsky equation as

$$\Delta W = qE_0T \cos fL \quad (23)$$

The physics contained within the transit-time factor is that the energy gain of a particle in a harmonically time-varying field is always less than the energy gain in a constant dc field equal to that seen by the particle at the center of the gap. The transit-time factor  $T$  is the ratio of the energy gained in the time-varying RF field to that in a dc field of voltage  $V_0 \cos \phi$ .

From the above, it is clear that the peak energy gain of a particle occurs when  $\phi=0$  and is  $\Delta W_{\phi=0}=qV_0T$ . The effective shunt impedance of a cavity is defined by

$$r = \left( \frac{\Delta W_{f=0}}{q} \right)^2 \frac{1}{P} = \frac{(V_0T)^2}{P} = r_s T^2 \quad (24)$$

This parameter in megohms measures the effectiveness per unit power loss for delivering energy to a particle. For a given field both  $V_0=E_0L$  and  $P$  increase linearly with cavity length, as do both  $r$  and  $r_s$ . For long cavities we often use a figure of merit that is independent of both the field level and the cavity length. Thus the shunt impedance per unit length  $Z$  is expressed as

$$Z \equiv \frac{r_s}{L} = \frac{E_0^2}{P/L} \quad (25)$$

Similarly, the effective shunt impedance per unit length  $ZT^2$  is

$$ZT^2 \equiv \frac{r}{L} = \frac{(E_0T)^2}{P/L} \quad (26)$$

$Z$  and  $ZT^2$  are usually tens of megohms per meter. One of the main objectives in accelerating cavity design is to choose the geometry to maximize effective shunt impedance per unit length. This is equivalent to maximizing the energy gain in a given length for a given power loss.

Another useful figure of merit is the ratio of effective shunt impedance to  $Q$ , often called  $r$  over  $Q$ ,

$$\frac{r}{Q} = \frac{(V_0T)^2}{wU} \quad (27)$$

$r/Q$  measures the efficiency of acceleration per unit stored energy at a given frequency. The effective shunt impedance per unit length is often used for  $r$  over  $Q$ , instead to quote the  $ZT^2/Q$ . These ratios are useful, because they are a function only of the cavity geometry and are independent of the surface properties that determine the power losses.

The multi-cavity traveling-wave structure can be viewed as a transmission line. If the energy stored in cell # $k$  is  $U_k$ , then the energy stored per unit length at  $z=z_k=(k-1)L$  is given by  $u(z_k)=U_k/L$ , with  $L$  the cell length. The power flowing past the point  $z$  is

$$P(z) = V_g u(z) \quad (28)$$

with  $V_g$  the local group velocity. In steady-state the energy density stored in one cell is constant in time, and thus

$$0 = \frac{dU}{dt} = (P_- - P_+) - \frac{w_0 U}{Q_w} \quad (29)$$

where  $Q_w$  is the wall  $Q$  of a single cell. The power flowing into the cell from the left is  $P_-$ , and the power flowing out is  $P_+$ . Thus,

$$P_- - P_+ \approx -L \frac{dP}{dz} = \frac{w_0 U}{Q_w} = \frac{w_0 u L}{Q_w} \quad (30)$$

or

$$\frac{dP}{dz} = -\frac{w_0 u}{Q_w} = \frac{d}{dz}(V_g u) \quad (31)$$

The structure we are studying here has the strictly periodic geometry. It forms a *constant impedance* structure.

The *shunt impedance per unit length* can be expressed as [6]:

$$Z_{TW} = \frac{Q_w}{L} \frac{(GL)^2}{w_0 U} = \frac{Q_w}{w_0 u} G^2 = \frac{G^2}{-dP/dz} \quad (32)$$

where  $G$  is the accelerating gradient, usually the peak axial electric field  $E_{z0}$  in traveling-wave accelerating structures. It is because that a particle should locate at a crest of the field and synchronizes with the wave propagation to obtain the maximum energy gain in a traveling-wave structure, and the peak energy gain of a particle is

$\Delta W_{\phi=0}=qE_z L$ . Consequently, the effective shunt impedance of a traveling-wave structure is the same as its shunt impedance.

One can also calculate the shunt impedance of a traveling-wave structure from the shunt impedance of the corresponding standing-wave structure [5]. The shunt impedance per unit length of a traveling-wave structure is twice the effective shunt impedance

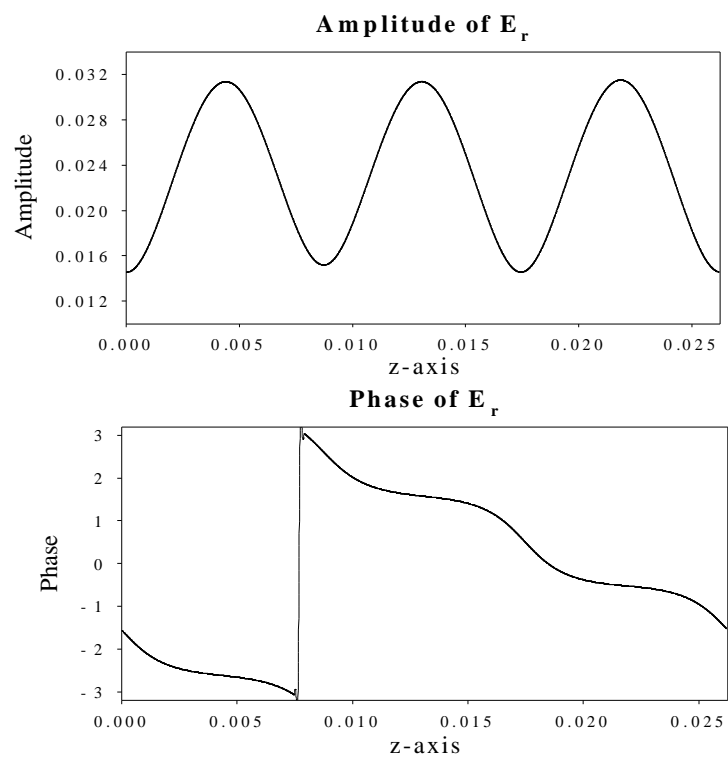
$$Z_{TW} = 2Z_{SW} T^2 \quad (33)$$

### III. CALCULATION RESULTS

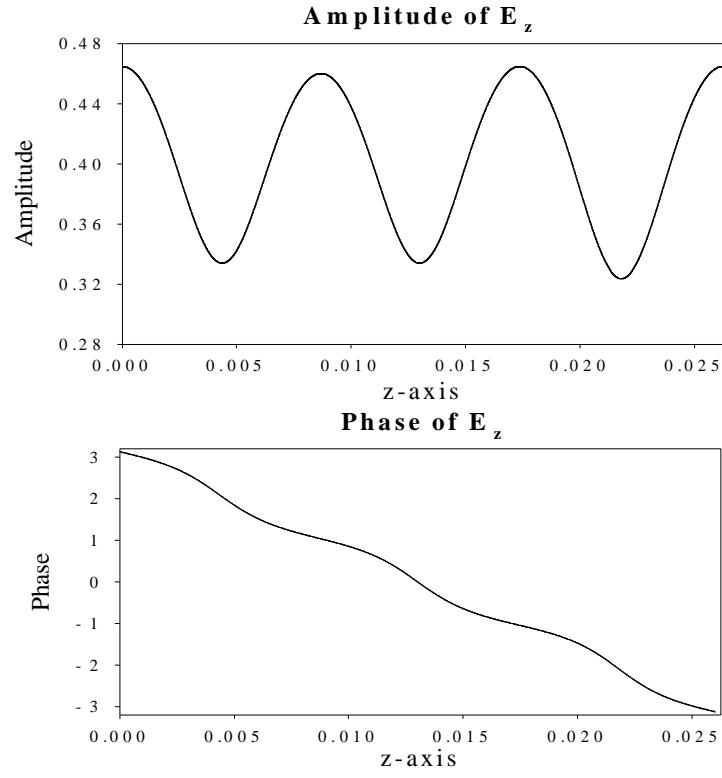
Here we are only interested in  $2\pi/3$  mode of the propagated wave, whose wavelength is equal to the total length of 3 cells when the phase velocity is the speed of light, because it has the maximum shunt impedance. First, we calculated a resonator with 3 cells with (Neuman boundary  $E_t=0$ ) using Eigenmode module of MAFIA. The field solutions and mesh coordinates can be output to ASCII data files. However, these data files are not ready for further calculations of the accelerator parameters we need. One post-processing program written in VC++ reads the field solutions and mesh information, filtering out unnumerical symbols in the input data files. This post-processing program also carries out the conversion from standing-wave solution to traveling-wave solution.

Fig. 3-5 show the plots of the amplitude and phase of  $E_r$ ,  $E_z$  and  $B_\phi$  that are obtained from the standing waves to traveling waves conversion in Equ. (10). They agree with the field characteristics of iris-loaded structures.





**FIGURE 2.**  $E_r$  at  $r=0.001\text{m}$  in the traveling-wave dielectric-iris loaded structure.



**FIGURE 3.**  $E_z$  at  $r=0$  in the traveling-wave dielectric-iris loaded structure.

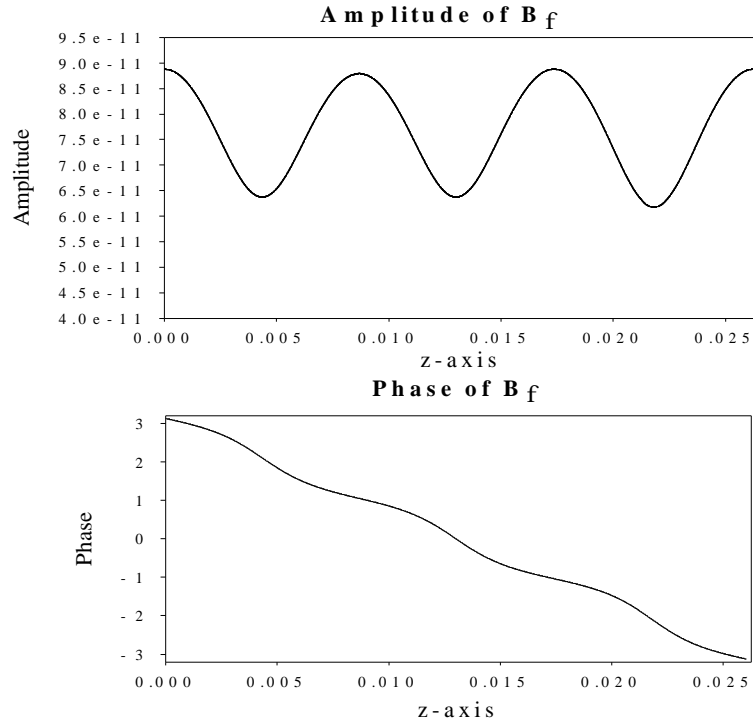


**FIGURE 4.**  $B_\phi$  at  $r=0.001\text{m}$  in the traveling-wave dielectric-iris loaded structure.

The electric field pattern of  $2\pi/3$  mode of the standing-wave dielectric-iris-loaded structure is shown in Fig. 5. This vector field plot is obtained from MAFIA simulation. It is generally agreed that the standing-wave field plot is one snapshot of the traveling wave at certain time  $t$ .

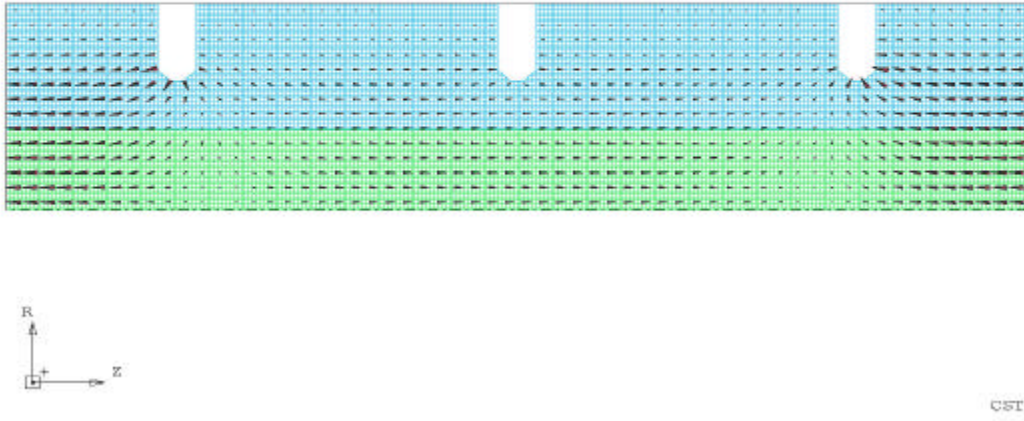


**FIGURE 5.** Electric field pattern of  $2\pi/3$  mode in dielectric-iris-loaded accelerating structure.

We chose a fixed beam hole with a radius of 4mm that is close to the typical beam hole size of NLC structures. Then the calculations have been carried out with varying the iris radius. Fig. 6 shows the iris radius vs. group velocity with filling different dielectric. From these curves, we can know the group velocity is almost determined by the size of iris instead of ceramic's dielectric constant. Fig. 7 illustrates this from another angle.

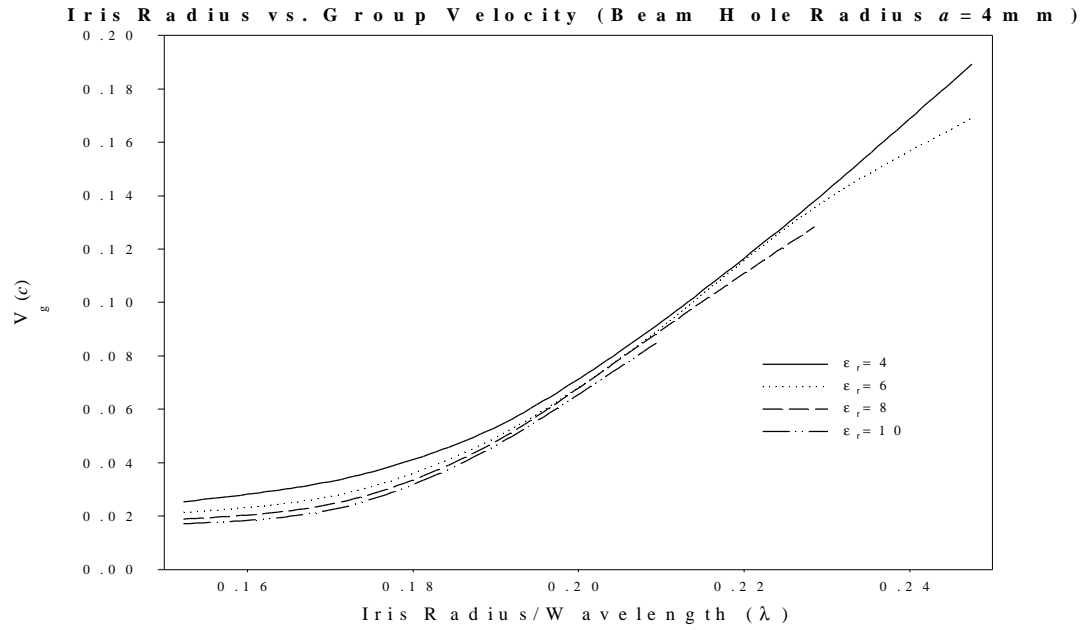


**FIGURE 6.** Iris Radius vs. Group Velocity for  $2\pi/3$  mode in dielectric-iris-loaded structure.

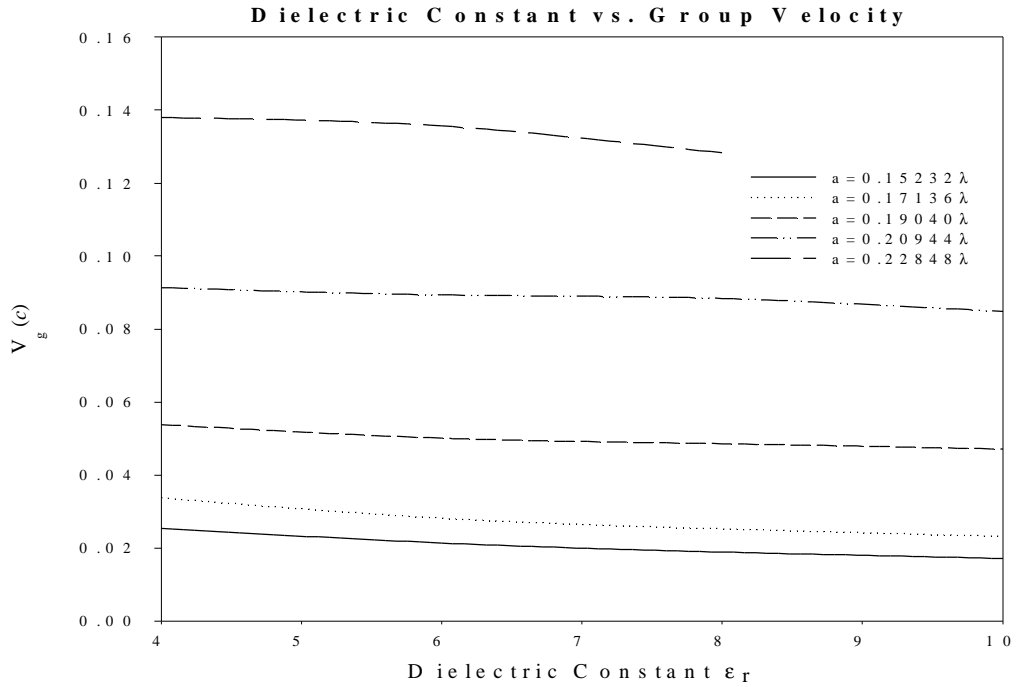


**FIGURE 7.** Dielectric constant vs. Group Velocity for  $2\pi/3$  mode in dielectric-iris-loaded structure.

A good accelerator usually needs a group velocity less than 10 percent of the speed of light in free space. However, there is not a universally applicable number on group velocity. In this case, the group velocity can be simply counted as a function of iris radius. We have to consider other parameters such as shunt impedance  $r$  and  $r/Q$  before choosing the size of iris, because these parameters also vary with the iris radius.

Fig. 8 shows how the shunt impedance per unit length of such traveling-wave structure is a function of iris radius and dielectric constant of filled ceramic.

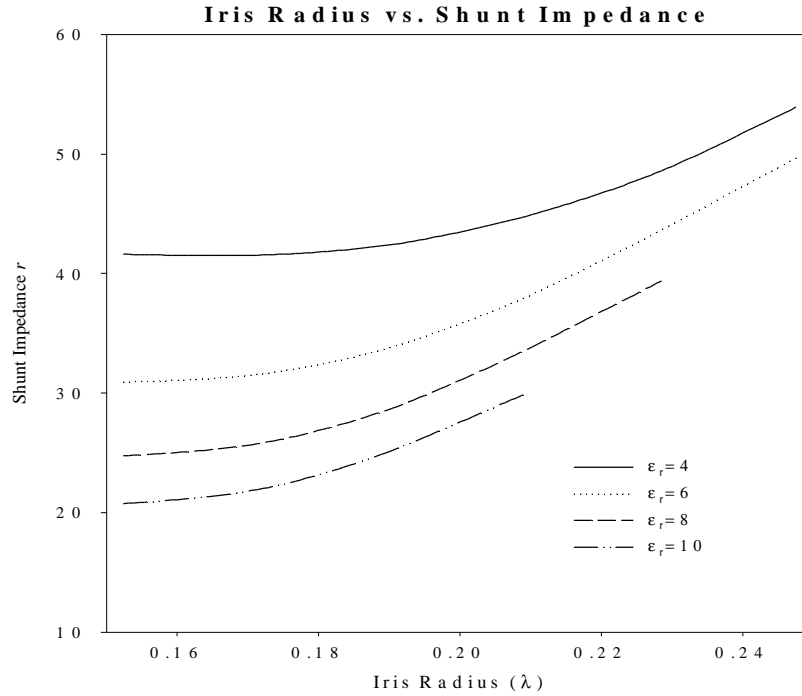


**FIGURE 8.** Shunt impedance per unit length of  $2\pi/3$  mode in dielectric-iris-loaded structure.

It is clear to say that the lower dielectric constant ceramic filling, the higher the shunt impedance per unit length. Moreover, the larger the iris, the higher the shunt impedance we have. Here we have to make a tradeoff between the group velocity and shunt impedance to reach an optimized iris radius. However, how to do such optimization is not an objective of this research.

Accelerators are also expected to have very high  $Q$ . Thus a given RF source can drive longer accelerating structures. Fig. 9 shows how  $Q$  varies with iris radius and dielectric constant.

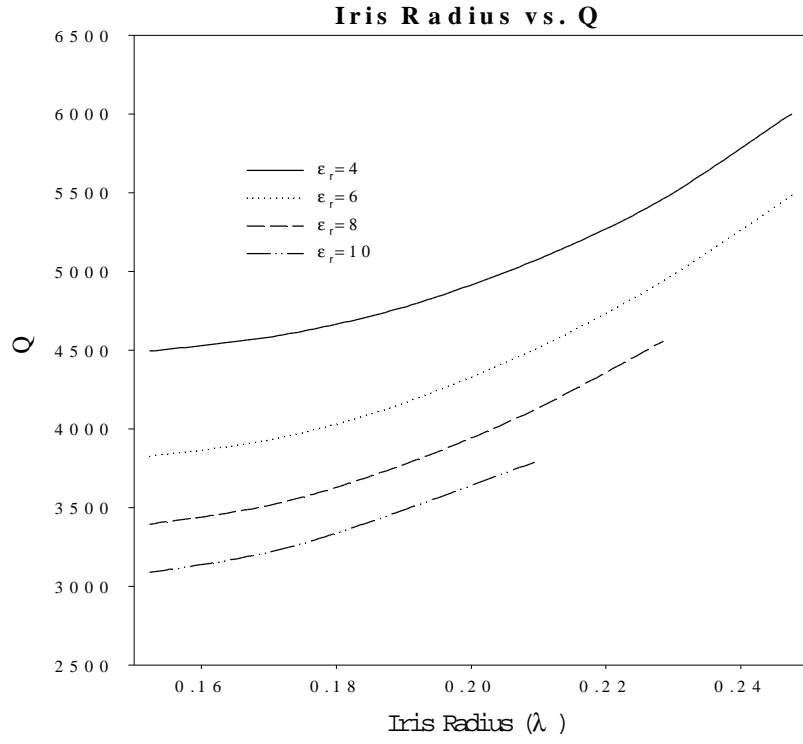


**FIGURE 9.** Quality factor of  $2\pi/3$  mode in dielectric-iris-loaded structure.

We can see the quality factor of dielectric-iris-loaded structures varies in the similar trend as the shunt impedance. For a given group velocity, we should choose ceramic with lower dielectric constant to have higher  $Q$ .

Another figure of merit of accelerating structure we should consider here is  $r/Q$ . It measures the acceleration efficiency for a given stored energy.

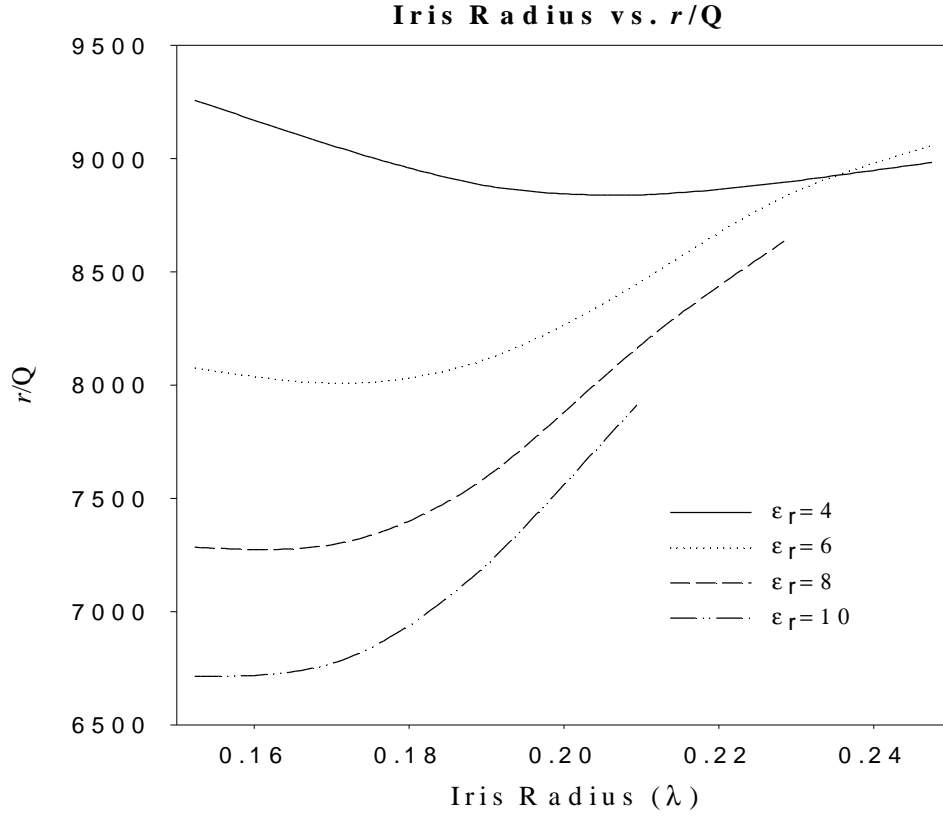


**FIGURE 10.**  $r/Q$  of  $2\pi/3$  mode in dielectric-iris-loaded structure.

The plot in Fig. 10 also shows ceramics with lower dielectric constant are preferred for achieving higher  $r/Q$ . When the size of irises is enlarged, the  $r/Q$  of such structure gets closer and closer to dielectric-lined circular waveguides. Considering achieving a relatively slow group velocity, increasing iris radius is not a good choice to enhance  $r/Q$ , because it causes faster group velocities.

The geometric parameters should be chosen with a comprehensive consideration to balance the requirements of shunt impedance,  $r/Q$ , and group velocity. We must take into consideration one more figure of merit  $E_s/E_{z0}$ . Reducing this ratio is the major drive for the studies of dielectric-iris-loaded structures. It is of great importance to know how the ratio of the peak surface electric field to the accelerating gradient varies with the size of irises and dielectric constant of ceramics. The plots of  $E_s/E_{z0}$  are shown in Fig. 11.

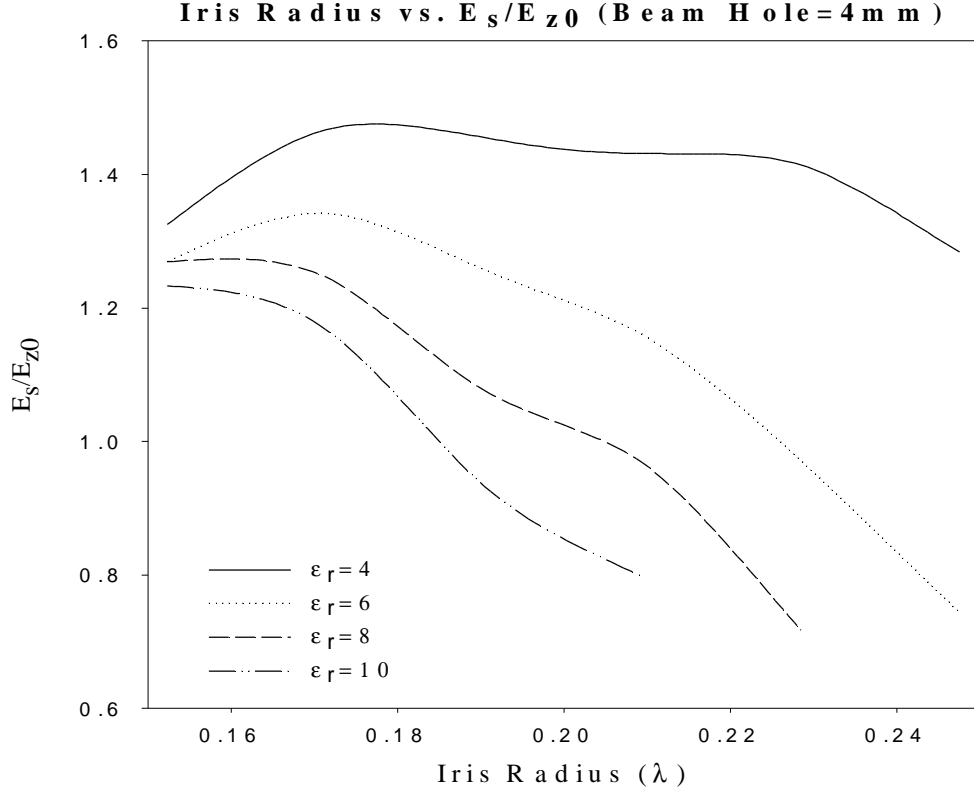


**FIGURE 11.**  $E_s/E_{z0}$  of  $2\pi/3$  mode in dielectric-iris-loaded structure.

If the dielectric constant of ceramic is greater than 6, the ratio of  $E_s/E_{z0}$  can be reduced dramatically with increasing dielectric constant. For dielectric constant materials with dielectric constant of 4, this ratio is reduced to less than 1.5. However, the amplitude of such change is small with varying the iris radius. From the trend of those curves in Fig. 11, we may draw a conclusion that  $E_s/E_{z0}$  may not be largely reduced using ceramics with dielectric constant less than 4, although dielectric-iris-loaded structures can certainly achieve less  $E_s/E_{z0}$  than conventional iris-loaded structures.

An optimization procedure can be applied to determine the optimal choice of iris radius and dielectric constant of ceramic to satisfy the requirements on  $E_s/E_{z0}$ , group velocity, shunt impedance,  $Q$ , and  $r/Q$ . Here we only compared the calculations already being made to pick one good choice. For a given beam hole radius of 4mm, the relatively good choice of iris radius and dielectric constant is listed in table 1. The corresponding accelerator parameters are also shown in this table.

**TABLE 1.** One set of parameters of dielectric-iris-loaded structure (beam hole radius=4mm)

Dielectric Constant	Iris Radius (mm)	$E_s/E_{z0}$	Shunt Impedance (MW/m)	$Q$	$r/Q$ (W/m)	Group Velocity $V_g$ (c)
6	5.5	1.1604	38.0633	4506	8446.873	0.089349



Comparing with NLC structure, the structure shown in table 1 has  $E_s/E_{z0}$  close to unity but lower shunt impedance. Meanwhile,  $r/Q$  is not dramatically lowered. It means this structure can have at least doubled accelerating gradient, but the efficiency of acceleration to the power dissipation is lowered. If we want to tolerate a little higher  $E_s/E_{z0}$ , the shunt impedance,  $Q$  and  $r/Q$  can be increased. How to choose these parameters depends on the design objectives. However, this kind of dielectric-iris-loaded structure can lower the ratio of peak surface electric field to peak accelerating gradient without losing much in other merits of accelerators.

Fig. 12 shows the contour plots and surface plot of the field amplitudes in the three cells of the dielectric-iris-loaded structure listed in table 1. We can easily identify that the peak surface electric field occurring at iris is very close to the peak axial electric field.

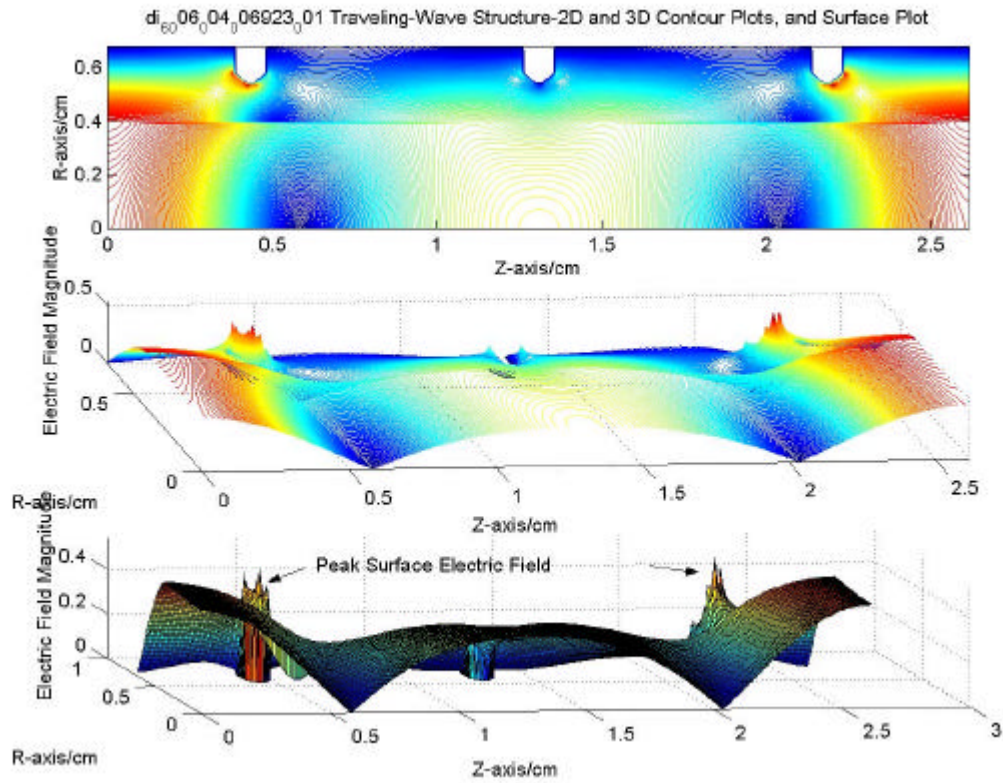


**FIGURE 12.** Traveling-wave electric field amplitude plots of  $2\pi/3$  mode in dielectric-iris-loaded structure at  $t=0$ .

#### IV. CONCLUSION

The analyses on dielectric-loaded periodic accelerating structures showed that the ratio of peak surface electric field to the maximum accelerating gradient in a traveling-wave structure can be reduce to unity without scarifying much in shunt impedance per unit length and quality factor. In other words, if high power RF sources are available, we can at least double the achievable accelerating gradient, comparing with that of conventional iris-loaded structures.

## REFERENCES

1. Flesher, G. and Cohn, G., *AIEE Transactions*, **70**, 1951, pp. 887-893.
2. Zhang, T-B., Hirshfield, J., Marshall, T., and Hafizi, B., *Physical Review E*, **56**, 1997, pp. 4647.
3. Chjonacki, E., Gai, W., Ho, C., Konecny, R., Mtingwa, S., Norem, J., Rosing, M., Schoessow, P., Simpson, J., *J. Applied Physics* **69**, 1991, pp. 6257.
4. Zou, P., Gai, W., Konecny, R., Sun, X., Wong, T., and Kanareykin, A., *Review of Scientific Instruments*, **71**, No. **6**, 2000, pp. 2301-2304.
5. Loew, G. A., Miller, R. H., etc., Computer Calculations of Traveling-wave Periodic Structure Properties, SLAC-PUB-2295, March, 1979.
6. Whittum, D. H., Introduction to Electrodynamics for Microwave Linear Accelerators, SLAC-PUB-7802, April, 1998.